 

*NANOOBJECTS*

PACS numbers: 78.67.Rb; 79.20.La
DOI: 10.1070/QE2014v044n03ABEH014774

# Optical response of alkali metal atoms confined in nanoporous glass*

A. Burchianti, C. Marinelli, E. Mariotti, A. Bogi, L. Marmugi,
S. Giomi, M. Maccari, S. Veronesi, L. Moi

*Abstract.* **We study the influence of optical radiation on adsorption and desorption processes of alkali metal atoms confined in nanoporous glass matrices. Exposure of the sample to near-IR or visible light changes the atomic distribution inside the glass nanopores, forcing the entire system to evolve towards a different state. This effect, due to both atomic photodesorption and confinement, causes the growth and evaporation of metastable nanoparticles. It is shown that, by a proper choice of light characteristics and pore size, these processes can be controlled and tailored, thus opening new perspectives for fabrication of nanostructured surfaces.**

***Keywords:*** *metal nanoparticles, porous glass, organic coating, laser-induced desorption, surface plasmon.*

## 1. Introduction

Interaction of light with matter produces numerous processes, most of which have been widely studied also thanks to the advent of lasers, at first, and, later on, to the availability of high coherent light intensities leading to nonlinear regimes. On the contrary, an increasing interest towards the phenomena triggered by a weak or very weak light intensity has been growing up in the last years aimed at finding new deep insights of unsolved problems and of their possible technological applications. The effect of light on adsorption and desorption processes is of great importance in the study of atom–surface interactions. The possibility to understand and to control the underlying mechanisms would have a remarkable impact: the ability to control atomic adsorption/desorption rates by light as well as nanoparticle growth on proper substrates or in proper environments is nowadays recognised as a promising technique in nanotechnology [1].

Exposure of a surface to light triggers many phenomena occurring at the interface and, as a consequence of atomic diffusion, also in the bulk. In this paper we present a detailed analysis of the effect of laser radiation on these processes. In this context, we focus our attention on light-induced desorption and cluster formation and evaporation of alkali metal atoms in porous glass matrices.

## 2. Light-induced atomic desorption

Atoms previously adsorbed into a porous substrate, as soon as light illuminates the adsorbing surface, are released into the vapour phase, thus creating an increase in the atomic density in confined volumes such as sealed glass cells. This phenomenon is observed also with weak (less than 1 mW $cm^{-2}$ ), incoherent and nonresonant light and is known as light-induced atomic desorption (LIAD) [2, 3].

LIAD is a nonthermal process, which is observed in many substrates such as organic films, quartz, glass, sapphire and stainless steel and with many atomic species such as alkali atoms and Ca (see review [4] and references therein).

Although LIAD is a general effect, which was also taken into account to explain the anomalous alkali atoms density in the atmosphere of the Moon [5], here we deal only with LIAD and related phenomena in porous glass samples exposed to alkali metal vapour contained in glass cells.

A major role in the LIAD phenomenon is played by the adsorption energy $E_{ads}$, which controls the microscopic interaction between the atoms and the surface. It is worth noting that the process involved can be described as physisorption, since the weak bonding between the atomic species and the substrate is due to an induced dipole which does not alter significantly the electronic structure of the adsorbed atom. Therefore, the atom can be 'retrieved' at any time through the proper mechanism and the proper energy.

Most materials like common glass have an adsorption energy of the order of 1 eV. This implies that many atoms are actually 'trapped' inside the surface with a low desorption probability: because of the relatively large desorbing energy only a few atoms can be actually removed and transferred into the vapour. On the contrary, organic films such as polydimethyl-siloxane (PDMS) exhibit an $E_{ads}$ of the order of 0.1 eV, thus offering a greater efficiency in photoejection of atoms: indeed, a surface of many square meters should be illuminated in the same experimental conditions in order to get a number of desorbed atoms comparable with the one obtained from a few squared centimetres of organic films. On the other hand, silica-based porous substrates present many advantages in terms of stability and repeatability of the characteristics and can be, in general, more easily handled than organic compounds. To solve this trade-off we suggested the use of nanoporous glass with an inner surface of 100 $m^2 g^{-1}$ [6]. In this way, the effective illuminated surface is quite large to compensate

*Reported at the XIX International Conference on Advanced Laser Technologies (ALT'11), Golden Sands, Bulgaria, September 2011.

**A. Burchianti, C. Marinelli, E. Mariotti, A. Bogi, L. Marmugi, S. Giomi, M. Maccari, L. Moi** CNISM and DSFTA, University of Siena, via Roma 56, 53100 Siena, Italy; e-mail: mariotti@unisi.it;
**S. Veronesi** CNISM and DSFTA, University of Siena, via Roma 56, 53100 Siena, Italy; NEST and Physics Department, University of Pisa, Largo Bruno Pontecorvo 3, 56127 Pisa, Italy

Received 4 November 2011; revision received 18 November 2013
*Kvantovaya Elektronika* **44** (3) 263–268 (2014)
Submitted in English

for the higher adsorption energy; as a consequence, a significant number of desorbed atoms are delivered by the sample.

## 3. Light-controlled processes in porous glass

Porous silica, commonly known also as porous glass, is obtained by chemically removing part of a glass mixture and thus leaving a porous silica skeleton ($SiO_2$ concentration is larger than 96%). The resulting samples contain an interconnected random network of narrow tunnels where atoms diffuse and can be adsorbed. In our experiments we used two different kinds of samples. The first one has pores with mean diameter of 17 nm, a free volume of 50% and a total pore surface of 100 $m^2$ $g^{-1}$. These porous glass samples are slides of $30\times15\times1$ $mm^3$ in size with an equivalent surface of about 40 $m^2$. In the following we will refer to this type of sample as PG. The second type of porous glass is a Vycor 7930 specimen supplied by Corning, indicated here as VPG. The tested samples are disks with a 11 mm diameter and 1 mm thickness. The mean diameter of the pores in this case is about 4 nm, the free volume is 28% and the equivalent surface is about 30 $m^2$.

With respect to PDMS coatings, PG and VPG do not exhibit the antirelaxation properties for which organic polymers [7] have been used, but present also a real chaotic distribution and interconnection of cavities. Moreover, unlike the case of PDMS coatings, in porous glass samples vapour phase atoms are confined in a small volume with a transverse dimension only 100 times bigger than the atomic size. Geometry and high irradiation of the surface are the main reasons for the peculiar behaviour of PG/VPG matrices with respect to organic coatings. Moreover, the direct comparison between the two different samples of porous glass is useful to further highlight the role of pore dimensions in the light-induced phenomena.

The porous glass samples are placed inside Pyrex cells containing a solid reservoir of an alkali metal; the whole cell is then kept at room temperature. The specimens are mechanically fixed by a Pyrex ring to the cell body.

Figure 1 shows a simplified scheme of a typical LIAD experiment with a PG sample in the presence of Rb vapours. A resonant laser beam crosses the cell volume allowing one to detect the atomic vapour density, while an IR laser beam monitors the sample transparency. The desorbing light, supplied by a third laser source, is sent to the sample through a telescope in order to obtain a homogenous illumination of the sample.

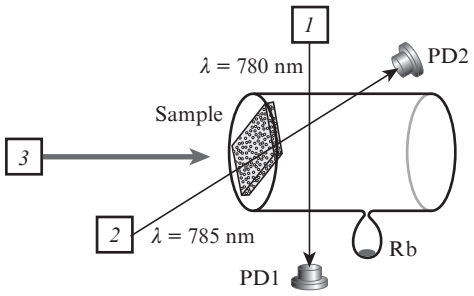


**Figure 1.** Scheme of the LIAD experiment for porous glass (PG or VPG) samples:
(*1*) density probe laser tuned on the $D_2$ line of Rb at 780 nm; (*2*) sample transparency monitoring laser diode at 785 nm; (*3*) desorbing light source (NIR and visible diodes or a cw doubled solid state Nd:YAG laser); (PD1 and PD2) photodiodes.

Upon illumination in the visible range, alkali atoms are quickly desorbed from the pores surface and thus ejected in the vapour phase because of the LIAD effect; as a consequence, the vapour density at room temperature is increased above the thermal equilibrium value, without any significant difference between the various alkali species such as Rb and Cs and with the same behaviour in the case of PG or VPG.

Figure 2 presents a relative density of Rb atoms as a function of time when a VPG sample is illuminated by visible desorbing light. At a given time $t = 0$, the desorbing light, which in this case is 50 mW $cm^{-2}$ at 532 nm, is switched on. In a few tens of ms, Rb atoms are desorbed from the porous sample, and thus the Rb atomic density is increased up to 120%. At $t = 115$ s the desorbing radiation is switched off and the density quickly drops to a lower value with respect to the equilibrium value, demonstrating a depletion of the porous glass sample. The starting equilibrium condition will be restored in a few hours.

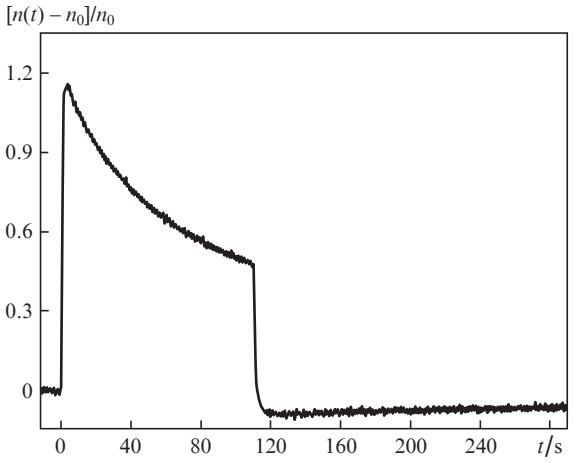


**Figure 2.** Relative vapour density of Rb atoms as a function of time. The desorbing light is delivered by a cw doubled Nd:YAG laser at 532 nm for 115 s. Laser intensity is 50 mW $cm^{-2}$ and uniform all over the VPG sample surface having pores 4 nm in size; $n_0 \approx 1.3\times10^9$ $cm^{-3}$ is the equilibrium density of Rb atoms.

We define the relative rate $R_n$ of the vapour density growth, immediately after the desorbing light is switched on at $t = t_0$, as follows:

$$R_n = \frac{1}{n_0}\frac{\mathrm{d}n}{\mathrm{d}t}\Big|_{t=t_0}.$$

The desorbing rate $R_n$ is mainly due to the atoms desorbed from the pores that are close to the outer sample surface. Figure 3 shows the dependence of $R_n$ on the desorbing photon energy in the case of PG contained in Rb vapour; results suggest the existence of two different desorption processes. One shows a monotonic increase in $R_n$ with increasing photon energy [curve (*2*) in Fig. 3]; the other one, instead, clearly exhibits a Gaussian-shaped resonance [curve (*3*) Fig. 3] in the near IR (NIR). The nonresonant contribution is due to LIAD from the porous surface while the resonant part is due to surface-plasmon induced desorption (SPID) from metallic

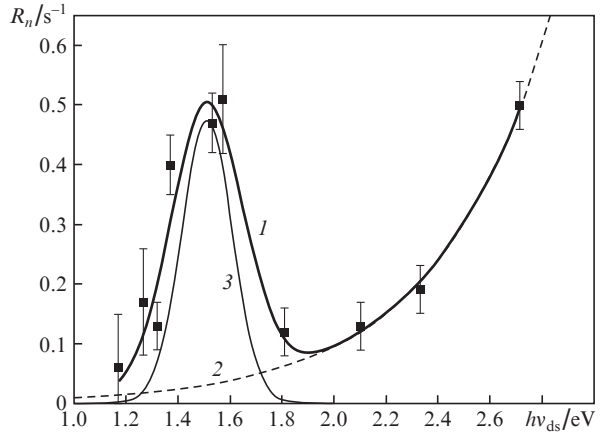


**Figure 3.** Desorption rate of Rb from PG having pores 17 nm in size as a function of desorbing photon energy $h\nu_{ds}$ at a light intensity of 5 mW cm$^{-2}$. Curve (*1*) is the best fit of the experimental data given by the sum of two contributions: one due to the LIAD effect (*2*) and one to the SPID effect from metallic clusters (*3*).

clusters which are formed inside the nanocavities by vapour diffusion in the dark [8, 9].

Evidence of metal cluster formation at the equilibrium inside the glass nanopores is found by recording the sample absorbance in the dark. Indeed, surface plasmon bands appear in porous glass samples exposed to alkali metal vapours. This feature is observed in both PG and VPG samples, as shown in Figs 4 and 5 [curves (*1*)], where the sample absorbance spectra are presented. Moreover, upon illumination with visible or UV light, a reversible modification in the optical properties of both samples is produced as proved by the absorbance changes: after illumination with a Hg lamp, the absorption peaks in the NIR region increase in intensity. Then, during relaxation in the dark, the sample absorbance comes back to its initial value in a few hours. The porous silica absorbance spectra are obtained by using a spectrophotometer. Once the cell is placed inside the instrument, the sample absorbance is recorded before and after sample illumination without removing the cell. This method allows us to evaluate the light-induced spectral change of the alkali metal-silica glasses avoiding spurious changes due to the cell alignment.

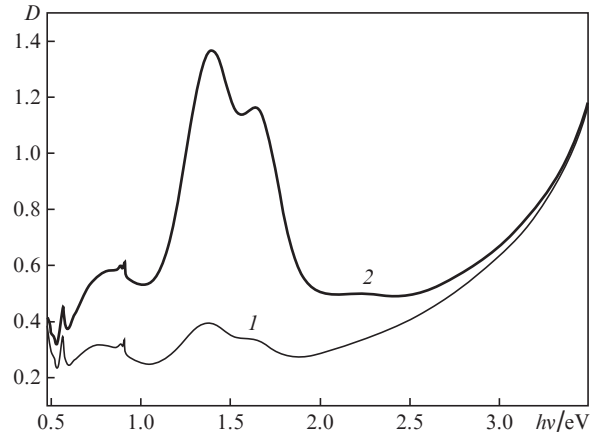


**Figure 4.** Absorbance of the PG sample having pores 17 nm in size: (*1*) absorbance at equilibrium after loading with Rb, (*2*) after 2 min exposure to a high-pressure Hg lamp at a light intensity of 10 mW cm$^{-2}$.

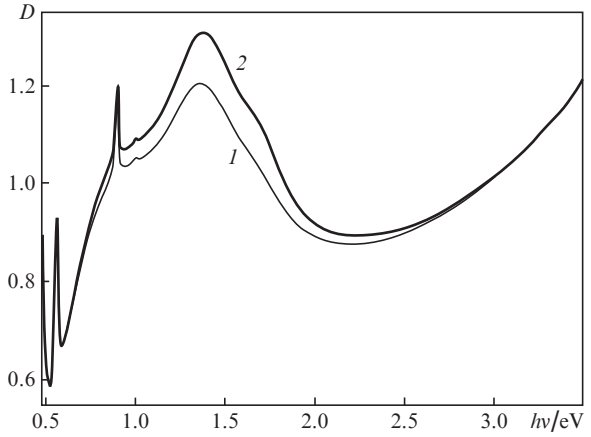


**Figure 5.** Absorbance of the VPG sample having pores 4 nm in size: (*1*) absorbance at equilibrium after loading with Rb, (*2*) after 2 min exposure to a high-pressure Hg lamp at a light intensity of 10 mW cm$^{-2}$.

The photo-induced changes in the optical properties of the PG/VPG sample can be ascribed to LIAD. In fact, because of the great number of adsorbed atoms and the relatively small volumes in which the vapour phase is confined, the probability of accumulation at surface defects is high and further increased upon visible illumination, which enhances the adsorbed atom mobility. As a consequence, LIAD is able to induce a systematic formation of metallic aggregates of alkali atoms, which remain on average stable for a time scale of several hours after the exposure to the desorbing light.

Results shown in Figs 4 and 5 demonstrate the presence of metallic nanoparticles formed in the dark or by the exposure to the desorbing light: the typical absorption bands in the NIR are the fingerprint of the metallic agglomerates, whose geometry and interaction with the dielectric substrate [10] determine the spectrum characteristics. In the case of PG loaded with Rb (Fig. 4), the two surface plasmon resonances located around $h\nu = 1.5$ eV are due to quasi-spherical clusters with the estimated mean radius of 3 nm, which is consistent with the pore size. The other observed absorption bands covering the entire optical spectrum are probably due to the formation of bigger metallic aggregates with different shapes. The main effect of the visible–UV illumination is, in this case, to increase the number of nano-sized spheroids inside the pores, as demonstrated by Fig. 4. Therefore, light in PG samples 'grows' particles with well-defined size and shape.

In Fig. 5, the absorbance of Rb-loaded VPG at the equilibrium in the dark is compared to the one recorded immediately after exposure to a high pressure Hg lamp light. In this case, the sample absorbance in the dark is higher than the one measured for Rb-loaded PG; this indicates a higher density of the metallic phase, due to the smaller free space inside the porous matrix. Moreover, bands due to the quasi-spherical nanoparticles are present also in this type of sample, even if they show peaks less resolved than the one in the previous case. This resonant bands broadening is caused both by a smaller mean particle size and a larger shape distribution. We must also notice that the positions of resonances are slightly red shifted: maximum resonance energy is 1.2 eV and 1.37 eV in the case of VPG and PG, respectively. A possible explana-

tion is a stronger interaction between single nanoparticles: in this case the pore size is only 4 nm and therefore the alkali clusters interact more due to the smaller average separation. The absorbance variation due to the illumination of the sample [curve (*2*) in Fig. 5] is one order of magnitude lower than in the case of PG having pores 17 nm in size, as a result of the smaller amount of nanoparticles grown up by light due to the reduced free volume in the sample.

A direct comparison of the optical response of these two kinds of porous glass after illumination is shown in Fig. 6. The relative absorbance variations in VPG with 4-nm pores and PG with 17-nm pores are very similar. This result shows that microscopic mechanisms of cluster growth by light are similar for both porous glass specimen and the only differences are due to cluster confinement geometry. The positions of the observed absorbance maxima after the exposure to desorbing light are coincident and both blue shifted with respect to the ones produced by nanoparticles formed in the dark. It is worth noting that the amount of this shift is different in the two glass samples: in the VPG sample the plasmon resonance is separated by 0.1 eV from the value measured in the dark and in the PG sample – by 0.02 eV. All these facts suggest that the light-induced nanoparticle production is similar in the two samples and that light builds up similar kinds of clusters, all less interacting, in both matrices and confirm that the major contribution to the absorbance of Rb absorbed in porous silica is due to nanoparticles smaller than the pore size. However, we can notice that the nanoparticles light-grown in VPG are slightly smaller than those in PG, since the two plasmon peaks are less resolved. This is in agreement with the different pore size of the two samples.

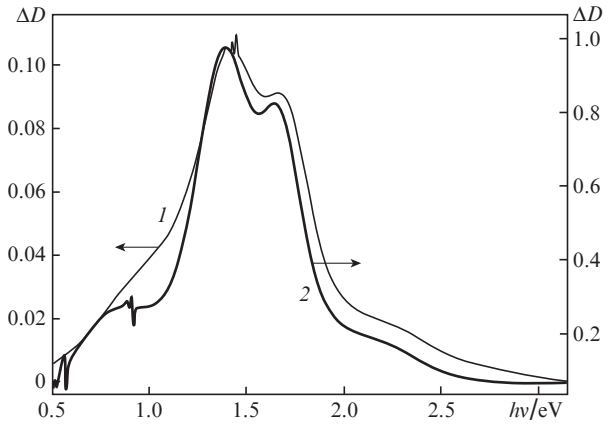


**Figure 6.** Comparison between the absorbances of VPG having pores 4 nm in size (*1*) and of PG having pores 17 nm in size (*2*) in the presence of Rb vapours after an illumination with a Hg lamp.

## 4. Erasable optical memory devices

Data presented in the previous section offer the possibility to realise a device with a controlled response to resonant light which can be tailored by a proper choice of the desorbing wavelength. The coexistence of the LIAD and the SPID effects can be exploited to create erasable light controlled optical memories.

As already discussed, exposure of the PG/VPG samples previously loaded with alkali atoms to UV-visible light induces the production of spheroidal nanoparticles and thus makes the sample opaque to red or NIR radiation. On the other hand, by illuminating the PG/VPG with resonant NIR radiation, it is possible to destroy the alkali clusters and therefore to make the sample transparent so that to probe radiation once again. In this case, as suggested in Fig. 1, the probe beam is actually a 'reading' beam, while the desorbing light is 'writing' radiation, when LIAD is induced, or 'erasing' radiation, when SPID is excited.

Figure 7 shows that the PG loaded with Rb can be used as a tool for reversible storing of images, by exploiting the proper sequence of desorbing radiation and the optical properties of

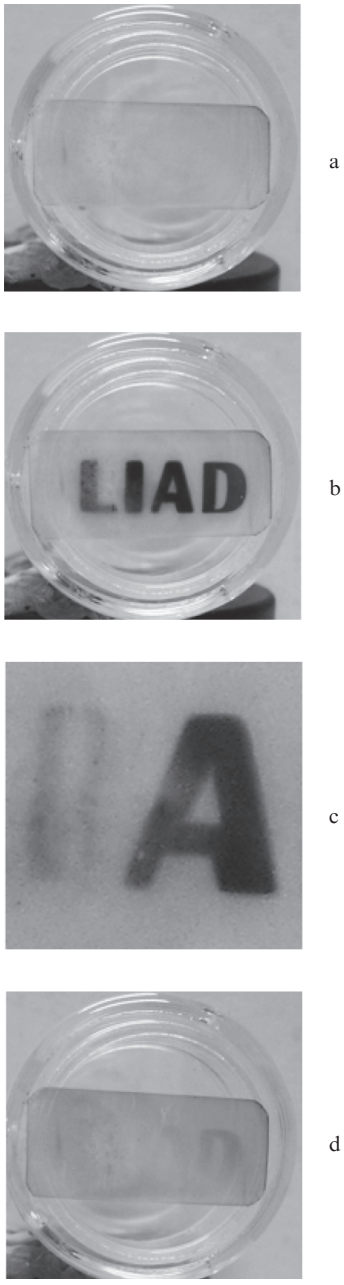


**Figure 7.** Light-controlled recording and storing of images with PG. Photographs of the PG sample loaded with Rb at various stages of the writing/erasing process: (a) sample at equilibrium; (b) after 2 min exposure to 20 mW $cm^{-2}$ at 532 nm; (c) bleaching of the central part of the letter 'I' by exposure to 2.7 W $cm^{-2}$ at 808 nm for 40 s; and (d) sample returns to equilibrium by relaxation in the dark [picture is taken 3 h after exposure to light (b)] [9].

the sample [9]. After exposure to 20 mW cm$^{-2}$ at 532 nm for 2 min, regions illuminated by the radiation are turned blue because of an increase in the number of Rb nanoparticles absorbing the red part of the visible spectrum. After this 'writing' phase, if the sample is exposed to resonant NIR, cluster evaporation is forced and thus the sample is bleached and its transparency is restored. Figure 7c shows the result after exposure to 2.7 W cm$^{-2}$ at 808 nm for 40 s of the central part of the 'I' letter. It is worth noting that the sample will eventually reach the initial condition if kept in the dark because of thermal evaporation of the light-induced clusters. In practice, as soon as the desorbing light is switched off, the dynamic equilibrium between evaporation and cluster formation created by the light itself is destroyed in favour of the first and the sample reaches the initial thermal equilibrium in a few hours (Fig. 7d).

The whole system exhibits also a 'memory effect', as a further demonstration of the interplay between LIAD, cluster formation and SPID. As shown in Fig. 8, the evolution of the nanoparticle population as well as the desorbed Rb vapour density are influenced by the previous status of the sample set by the previous illumination.

In details, two subsequent pulses of NIR (808 nm) radiation separated by 500 s have no appreciable difference in the transparency of the sample or in the Rb vapour density. However, if between the two red pulses, the sample is exposed to blue radiation at 488 nm, the response to the second NIR pulse is significantly different from the previous case: PG sample transparency significantly increases rather than showing a small decrease and the vapour density enhancement is, in this case, more than 30% larger.

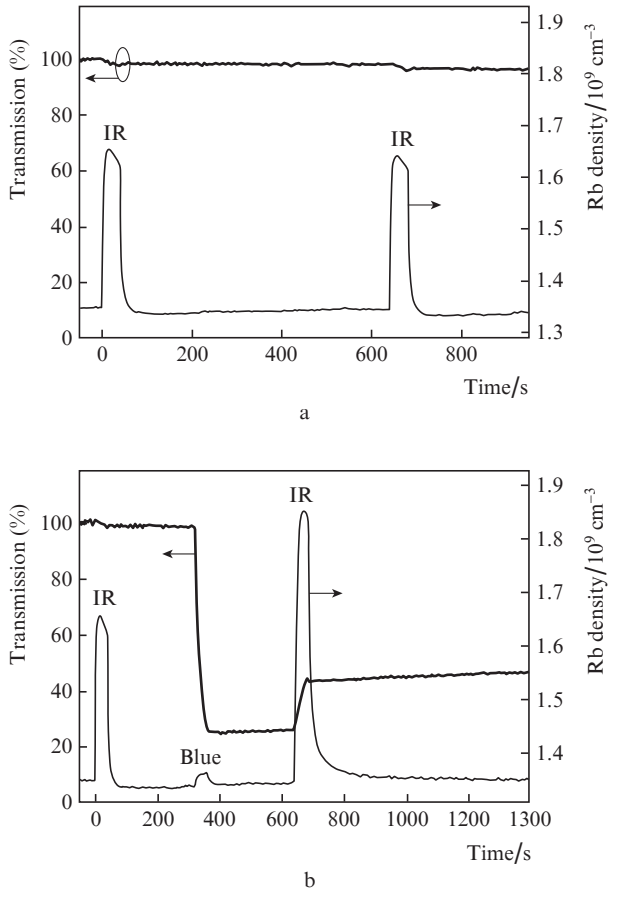


**Figure 8.** PG memory effect: different responses are observed with different illumination sequences: (a) PG sample transmission at 785 nm and Rb vapour density evolution with two subsequent exposures to 2.2 W cm$^{-2}$ at 808 nm and (b) same PG sample response to a sequence at 808 nm (2.2 W cm$^{-2}$), 488 nm (5.6 mW cm$^{-2}$) and 808 nm (2.2 W cm$^{-2}$) [9].

Such behaviour is explained once again by the interplay between the light-triggered phenomena at pore inner surfaces: blue light is capable of producing an efficient desorption of adsorbed atoms via LIAD. This, as already discussed, causes a high probability of agglomeration for atoms in the vapour phase and thus the production of metal nanoparticles inside the porous matrix: the transparency of the sample at 785 nm is thus progressively decreased. With respect to the first 'shot', the optical response of the sample exposed to the second cycle of NIR radiation is very different: although the vapour density has already returned to the equilibrium value, a large number of NIR absorbing Rb clusters is still present inside the PG, because of the relatively slow thermal evaporation. Thus, 808-nm radiation of the second 'shot' is strongly adsorbed by blue-induced clusters, which are then forced to evaporate by SPID. As a consequence, some of the clusters are rapidly destroyed and atoms are desorbed into the vapour phase: the transparency of the sample increases and the vapour density exceeds the value obtained with the previous exposure to NIR, as clearly shown in Fig. 8.

## 5. Conclusions

Our investigation on desorption processes in porous glass (PG) and Vycor porous glass (VPG) samples loaded with alkali atoms demonstrated the coexistence of two different light-driven mechanisms: one is the well-known nonresonant LIAD effect, while the second has a resonant character and is due to the excitation of surface plasmons at the interface between the silica substrate and the metallic nanoparticles formed inside the pores thanks to the small diameter (17 nm or 4 nm). It was demonstrated how, by a proper choice of illumination in the visible or in the near-IR spectrum, it is possible to control and to manipulate the population of spheroidal nanoparticles in a complete reversible way; as a result, the optical properties of the system can be tailored and controlled. Moreover, a memory effect depending on the particular sequence of illumination was demonstrated and explained with the result of the interplay between the two desorbing mechanisms LIAD and SPID.

In conclusion, the unique characteristics of the porous glass matrices allow both for an efficient desorption induced by light, but also for some unexpected behaviour related to the creation, in turn induced by light, of metal nanoparticles inside the host sample. It is clear how dimensionality and geometry of the system play a key role in allowing this phenomenon. Moreover, by a proper choice of illumination sequences, it is possible to tailor the interplay between the non resonant LIAD effect and the resonant SPID effect in order to control the optical response of the glass sample. This opens new perspectives for a light-controlled optical memory and also for the manipulation of metal nanoparticles in disordered media.

## References

1. Emel'yanov V.I. *Kvantovaya Elektron.*, **36**, 489 (2006) [*Quantum Electron.*, **36**, 489 (2006)]; Tarasenko N.V., Butsen A.V. *Kvantovaya Elektron.*, **40**, 986 (2010) [*Quantum Electron.*, **40**, 986 (2010)];

Izgaliev A.T., Simakin A.V., Shafeev G.A. *Kvantovaya Elektron*., **34**, 47 (2004) [*Quantum Electron.*, **34**, 47 (2004)].
2. Gozzini A., Mango F., Xu J.H., Maccarrone F., Bernheim R.A. *Nuovo Cimento Soc. Ital. Pis. D*, **15** (5), 709 (1993).
3. Meucci M., Mariotti E., Bicchi P., Marinelli C., Moi L. *Europhys. Lett*., **25** (9), 639 (1994).
4. Burchianti A., Bogi A., Marinelli C., Mariotti E., Moi L. *Phys. Scr. T*, **135**, 014012 (2009).
5. Yakshinskiy B.V., Madey T.E. *Nature*, **400**, 642 (1999).
6. Burchianti A., Marinelli C., Bogi A., Brewer J., Rubahn K., Rubahn H.-G., della Valle F., Mariotti E., Biancalana V., Veronesi S., Moi L. *Europhys. Lett*., **67**, 983 (2004).
7. Bouchiat M.A., Brossel J. *Phys. Rev*., **147**, 41 (1966).
8. Burchianti A., Bogi A., Marinelli C., Maibohm C., Mariotti E., Sanguinetti S., Moi L. *Eur. Phys. J. D*, **49**, 201 (2008).
9. Burchianti A., Bogi A., Marinelli C., Mariotti E., Moi L. *Opt. Expre*ss, **16** (2), 1377 (2008).
10. Gans R. *Ann. Phys.*, **47**, 270 (1915).